International Conf. On Advanced Robotics (ICAR) 2005, July 18-20, 2005 Seattle, WA, USA

Towards AGV Safety and Navigation Advancement - Obstacle Detection using a TOF Range Camera*

R.V. Bostelman, T.H. Hong, and R. Madhavan

***Abstract*— The performance evaluation of an obstacle detection and segmentation algorithm for Automated Guided Vehicle (AGV) navigation using a 3D real-time range camera is the subject of this paper. Our approach has been tested successfully on British safety standard recommended object sizes and materials placed on the vehicle path. The segmented (mapped) obstacles are then verified using absolute measurements obtained using a relatively accurate 2D scanning laser rangefinder. Sensor mounting and sensor modulation issues will also be described through representative data sets.**

***Index Terms*—3D range camera, real-time, safety standard, ground truth, obstacle segmentation.**

I. INTRODUCTION

Obstacle detection and mapping are crucial for autonomous indoor driving. This is especially true for Automated Guided Vehicle (AGV) navigation in factory-like environments where safety of personnel and that of the AGV itself is of utmost importance. This paper describes the performance of an obstacle detection and segmentation algorithm using a 3D real-time range camera.

The 3D range camera is based on the Time-Of-Flight (TOF) principle [8] and is capable of simultaneously producing intensity images and range information of targets in indoor environments. This range camera is extremely appealing for obstacle detection in industrial applications as it will be relatively inexpensive as compared to similar sensors and can deliver range and intensity images at a rate of 30 Hz with an active range of 7.5 m while incorporating no moving parts, such as a spinning mirror as in many off-the-shelf laser sensors.

Since obstacle detection plays a critical role in autonomous driving, there has been much research on many different types of sensors, such as sonar [13], color/gray level cameras [2], FLIR (Forward Looking InfraRed) cameras [12], and stereo cameras [11], [1], [14], [6]. Most of the vision approaches are not applicable to indoor scenes due to lack of texture in the environment. Other researchers have proposed LADAR (Laser Detection And Ranging) sensors for detecting obstacles [4], [3], [5]. However, one-dimensional LADAR, which has been used in the AGV industry, is not suitable for the 3D world of factory environments and other complex volumes without moving the sensor during operation.

Our proposed approach to obstacle detection uses a low cost, 3D, real-time, range camera. First, we calibrate the camera with respect to the AGV so that we can convert the range values to 3D point clouds in the AGV coordinate frame. Second, we segment the objects which have high intensity and whose elevation values are above the floor of the operating environment on the AGV path. The segmented 3D points of the obstacles are then projected and accumulated into the floor surface-plane. The algorithm utilizes the intensity and 3D structure of range data from the camera and does not rely on the texture of the environment. The segmented (mapped) obstacles are verified using absolute measurements obtained using a relatively accurate 2D scanning laser rangefinder. Our approach has been tested successfully on approximate British safety standard recommended object sizes covered with cotton, cloth material and placed on the vehicle path. The AGV remained stationary as the measurements were collected for this paper.

The U.S. American Society of Mechanical Engineers (ASME) B56.5-2004 standard [15] was recently upgraded[1] to allow non-contact safety sensors as opposed to contact sensors such as bumpers to be used on AGVs. Prior to the upgrade, the B56.5 standard defined an AGV bumper as a "mechanically actuated device, which when depressed, causes the vehicle to stop." With the current B56.5 standard upgrade and with state-of-the-art non-contact safety sensors, vehicles can be shorter in length, excluding mechanical bumpers since these bumpers extend much farther in front and behind the vehicle than non-contact sensors. This in turn allows shorter vehicle turning radii and they can potentially move faster as objects can be detected well before the vehicle is close to an object.

Ideally, the U.S. standard can be upgraded even further similar to the British EN1525 safety standard requirements [16]. Furthering the US safety standard will also provide support toward a unified, global safety standard for AGV's and other driverless vehicles.

Manuscript received November 16, 2004.

R.V. Bostelman is with the National Institute of Standards and Technology, Gaithersburg, MD 20899 USA (phone: 301-975-3426; fax: 301-921-6165; e-mail: roger.bostelman@nist.gov).

T.H. Hong is with the National Institute of Standards and Technology, Gaithersburg, MD 20899 USA (e-mail: tsai.hong@nist.gov).

R. Madhavan is with the National Institute of Standards and Technology, Gaithersburg, MD 20899 USA (e-mail: raj.madhavan@nist.gov).

* Commercial equipment and materials are identified in this paper in order to adequately specify certain procedures. Such identification does not imply recommendation or endorsement by the National Institute of Standards and Technology, nor does it imply that the materials or equipment identified are necessarily the best available for the purpose.

[1] not cited here since the upgrade was not published prior to the date of this paper.

The paper has five sections: Section II describes the concept of obstacle detection and segmentation including the 3D range camera, algorithm, and a modulation issue using range camera images. Section III provides the experimental setup and results when the proposed algorithm is employed for detection and segmentation of British standard size and material-covered test apparatus. Section IV provides further discussion beyond the typical indoor factory environment application and indicates future research areas that are under investigation including sensor mounting and outdoor daylight tests and results. Section V provides a summary and conclusion followed by acknowledgments and a reference list.

II. Obstacle Detection and Segmentation

A. 3D Range Camera

In this section, we describe an algorithm to detect and segment obstacles in the path of the AGV using a solid-state Time-Of-Flight (TOF) range camera. The 3D range camera shown in Figure 1 is a compact, robust and cost effective solid state device capable of producing 3D images in real-time.

Figure 1 - CSEM SwissRanger-2 3D Range Camera. *The camera simultaneously generates intensity images and range information of targets in its field-of view at a rate of 20 Hz with an active range of 7.5 m.*

The camera measures 14.5 x 4 x 3 cm (5.7 x 1.6 x 1.2 in), has a field-of-view of 42° (horizontal) x 46° (vertical), and is capable of producing range images of 160 x 124 pixels over a 7.5 m range. For a brief overview of the characteristics and operating principles of the camera, see [10].

The British EN1525 safety standard specifies that horizontal test pieces used to test sensors shall be 200 mm diameter x 600 mm long lying perpendicular to the vehicle path. Vertical test pieces shall be 70 mm diameter by 400 mm tall and completely within the vehicle path. Approximately sized British standard test obstacles, as shown in Figure 2 a and b, were placed on the travel path for our experiments.

B. Algorithm Details

Generally, the obstacle detection and segmentation algorithm combines intensity and range images from the range camera to detect the obstacles and estimate the distance to the obstacles. We first calibrate the camera with respect to the AGV so that we can convert the range values to 3D point clouds in the AGV coordinate frame.

(a)

(b)

Figure 2 - *Experimental setup (a) vertical test apparatus where the center object most closely matches the British standard size test piece measuring 65 mm dia. x 400 mm long. The remaining vertical objects are all thinner. (b) horizontal test apparatus (mannequin leg) measuring a segment approximately tapered from 80 to 160 mm dia. x 600 mm long including the leg ankle to the thigh. Both (a) and (b) objects are covered in cloth as also specified in the standard. See Section III Experimental Setup and Results for further details.*

Next, we segment the objects which have high intensity pixels and whose elevation values are above the floor of the operating environment on the AGV path. The segmented 3D points of the obstacles are then projected and accumulated into the floor surface-plane. The algorithm utilizes the intensity and 3D structure of range data from the camera and does not rely on the texture of the environment. The segmented (mapped) obstacles are verified using absolute measurements obtained using a relatively accurate 2D scanning laser rangefinder.

Specifically, the steps of the algorithm are illustrated for a sample image from the camera:

1) a patch of data (e.g., 20 x 20 pixels) with high intensity values (i.e., the intensity value is greater than 20) in front of the robot are used to fit a plane for estimating the floor surface as shown in Figure 3(a).

2) the left and right edges of 3D robot paths are projected to the range and intensity images such that only obstacles on the path can be considered as shown in Figure 3(b).

3) all the intensity pixels between the left and right edges are used to hypothesize the potential obstacle. If the pixel intensity value is greater than half of the average of the intensity in the image then the pixel is considered as a potential obstacle as shown in Figure 3(c).

4) each potential obstacle pixel in the range image is used to find the distance to the floor plane when the distance to the floor is greater than some threshold as shown in Figure 3(d). The threshold is dependent on the traversability of the robot.

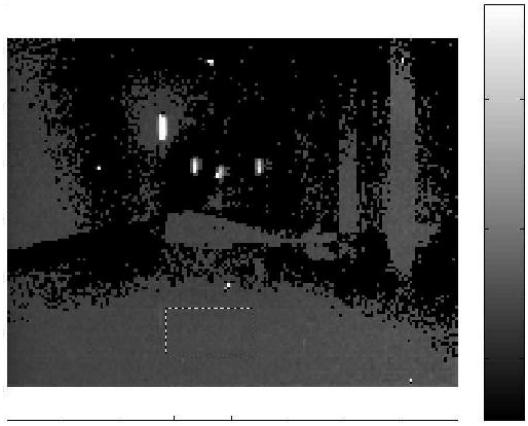

(a)

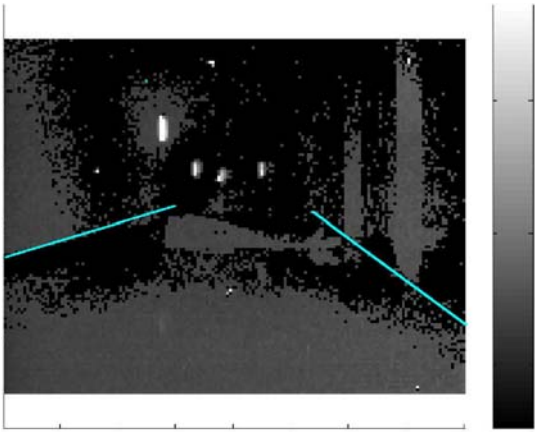

(b)

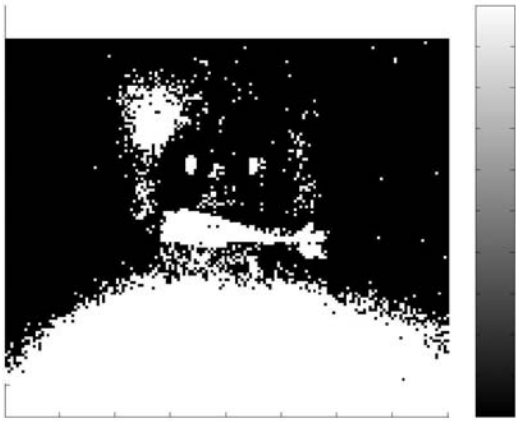

(c)

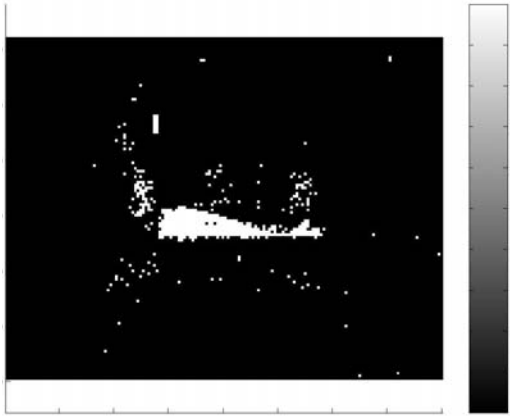

(d)

Figure 3 - *Obstacle segmentation algorithm illustration.*

Potential obstacles in the world model can be accumulated as the AGV drives. Figure 4(b) shows an obstacle map representation that is part of the world model. The obstacles map is shown at 10 cm grid resolution. Nearly all the obstacles are found, although at the cost of false positives from the reflected objects. To increase the accuracy of obstacle detection, the obstacles in the map and information obtained from an added color camera may be temporally integrated. Such integration has proven to be a very useful cue for obstacle detection [9].

C. Modulation Issue

An issue with this particular range camera is the modulation of returned data at approximately 7.5 m. Within the range of approximately 7.5 m, the camera accurately senses (to within 5 mm) the range to objects. Beyond 7.5 m, the camera continues to sense objects although places the object within the modulation of 7.5 m. For example, an object detected at 11 m would be placed in the returned data at a range of (11 m – 7.5 m =) 3.5 m (see Figure 4).

To eliminate the modulation issue, a lower emitted light modulation frequency (ELMF) below the typical 20 MHz can be used to establish a longer, yet lower accuracy (as stated by the manufacturer) range modulation and could be used to compare with the 7.5 m range modulated range data. The compared data within the two modulation frequencies can then be used to mask objects detected beyond the 7.5 m range. Also, similar to how humans have and use peripheral vision, these longer-range objects created by a higher ELMF setting, could be placed in the world model for additional, lower range-accuracy environmental information. And as human peripheral vision provides excellent motion detection over foveal vision [7], the higher ELMF setting could produce low relative accuracy, yet larger range and volume (see Figure 5) motion detection of obstacles. While the disadvantage here is producing lower relative range accuracy, the advantage for vehicle control is that decisions can be made much earlier to react to potential obstacles farther away, even if their exact range is unknown.

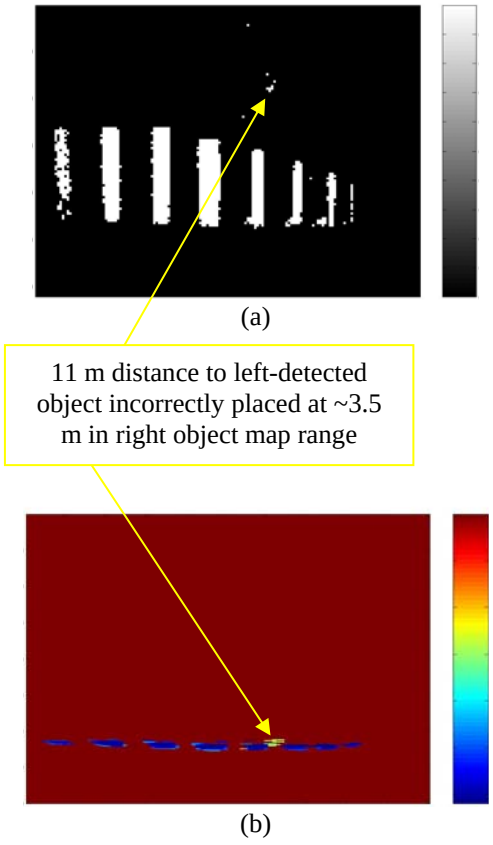

Figure 4 *– (a) Segmented obstacles and (b) obstacle map but, due to range modulation, obstacles detected beyond 7.5 m max. camera range are placed within the 7.5 m range.*

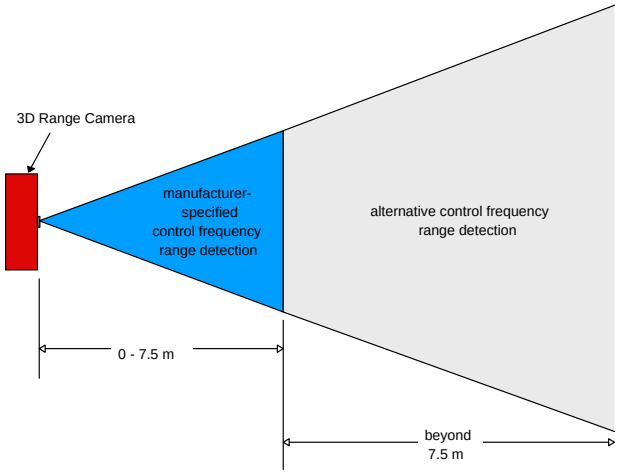

Figure 5 *– Graphic depicting range information (left) versus potential range information (right) with an alternative emitted light modulation frequency.*

III. EXPERIMENTAL SETUP AND RESULTS

The experiments were conducted under two scenarios as stated within the European British Standard:

- A test apparatus with a diameter of 200 mm and a length of 600 mm placed at right angles on the path of the AGV.
- A test apparatus with a diameter of 70 mm and a height of 400 mm set vertically within the path of the AGV.

Figures 2(a) and (b) show the experimental setup for the two aforementioned scenarios. The center of the camera lens was centered approximately horizontal and vertical on the apparatus for all measurements. The scanning laser rangefinder was offset from the camera by 0 mm horizontally, 250 mm vertically, and to the left of the camera as viewed from the camera to the test apparatus. The range camera was used to detect known test apparatus mounted on a stand and moved to different locations with respect to the camera.

The obstacle detection and segmentation algorithm was tested on two British standard test apparatus' as described in [15], and was evaluated against ground truth and placed at 0.5 m to 7.5 m distances to the sensor. A single-line scanning laser rangefinder, shown in Figure 6, mounted below the range camera, simultaneously verified the distance to the test apparatus for each data set and served as ground truth. The rangefinder produced 401 data points over a 100° semi-circular region in front of the robot with each scan.

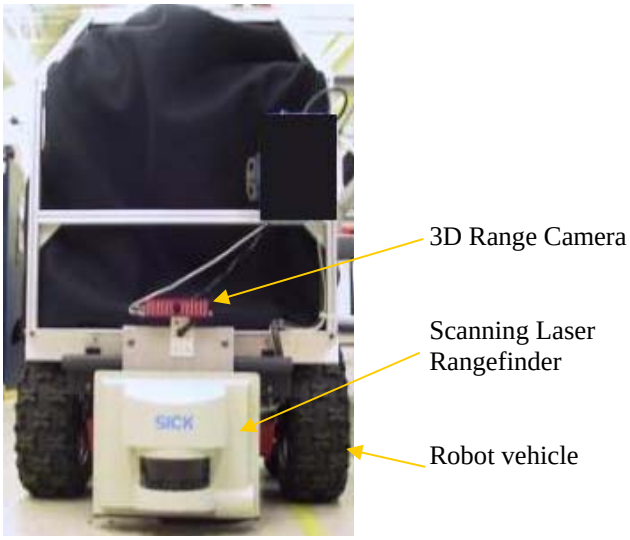

Figure 6 - *Experimental setup of the AGV, the scanning laser rangefinder, and the range camera.*

Table 2 shows the performance of the range camera for detecting the distance to the test apparatus placed at several distances from the range camera. As can be seen, the accuracy (mean) of the range decreases as the distance of the apparatus placed in front of the range camera is increased.

Figure 7 shows the test apparatus placed at a distance of 2.5 m from the range camera. Each object in the test apparatus was clearly detected even though the range camera detected the reflectors on the hallway wall. Figures 7 (a), (b) and (c) shows the resultant intensity, range, and segmented images, respectively. Figure 7(d) shows the ground truth provided by

the scanning laser rangefinder rotated to show a top-down view.

Table 2 Quantitative Comparison of Performance

Nominal Obstacle Distance (cm)	*3D Range Camera Mean (cm)*	*2D Rangefinder Mean (cm)*
64	64.076	64.662
111	111.039	111.316
160	161.390	160.690
210	204.004	210.000
259	249.499	259.143
310	284.703	310.158

Similar to Figure 3, [9] shows additional data taken with a mannequin leg placed on the floor and with an approximate diameter of 200 mm and a length of 600 mm at the leg thigh region. This test apparatus is more challenging for the algorithm because the entire object is close to the floor. The legs are detected, but at the cost of detecting farther objects. Again, this deficiency can be eliminated by using two different modulation frequencies (such as 10 MHz and 20 MHz) where the detected objects would be coarsely represented at a more appropriate distance. The control algorithm can then intelligently delete them.

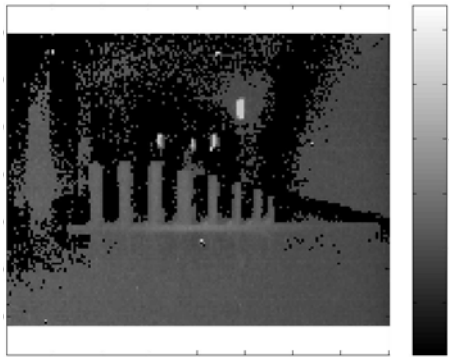

(a)

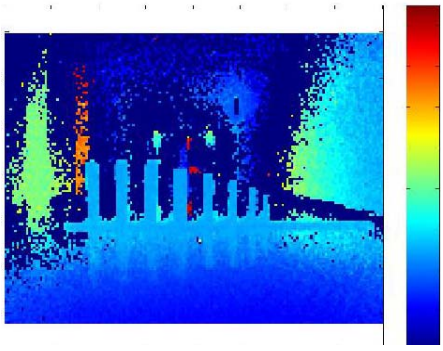

(b)

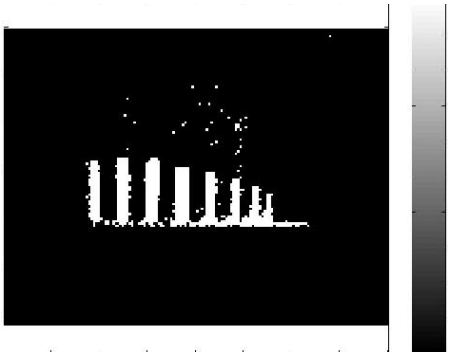

(c)

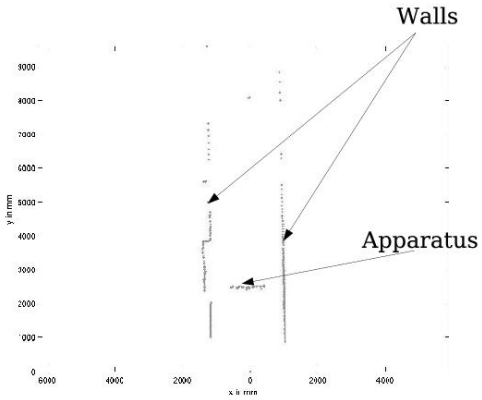

(d)

Figure 7 - *Results of the obstacle detection and segmentation algorithm for the experimental setup shown in Figure 2(a). The resultant intensity, range, and segmented images are shown in (a), (b) and (c), respectively. The ground truth provided by the scanning laser rangefinder is shown in (d) and has been rotated to show a top-down view.*

IV. FURTHER RESEARCH

A. Sensor Mount

Critical to the sensor itself is the mounting configuration of the sensor to enable detection of objects within the vehicle path. Although there are no specific guidelines within the US safety standard for sensor mounts, it does suggest that the sensor be “fail-safe” and regarding bumpers, they “shall activate from a force applied parallel to the floor.” Fix-mounting the sensor with its’ view in the direction of vehicle travel seems ideal where for example, a sensor that was mounted on perhaps a rotary head might possibly not detect an approaching obstacle outside the rotated FOV (field of view). A range camera fix-mounted on the vehicle and near the floor is also ideal where reflected data off the floor is less likely to detect the floor as an object. However, taller vehicles may require the need to view higher volumes as overhead objects may be within the vehicle path. Similarly, AGV’s typically have sensors that detect objects such as human feet to the side of the vehicle. Non-contact safety sensors must therefore, wrap their FOV around the vehicle or duplicate sensors, especially as camera prices decrease, to incorporate these potentially hazardous regions.

Figure 8 shows one possible configuration of 3D range cameras mounting locations to detect not only in front of the vehicle but, also to the sides. This concept could have potential detection issues that may be simply solved by timing the light emission from each camera to consecutively, as opposed to simultaneously, enable light emission and detection from the sensor. For example, camera 3 could be turned on, collect data, and turn off before camera 4 senses emission from camera 3 and cycled fast enough to stop the vehicle in an emergency. NIST currently controls the camera at 30 Hz. Moreover, cameras 1, 2 and 5, 6 could be combined from independent camera FOV's into a dual camera FOV. Additionally, the side cameras could be added too.

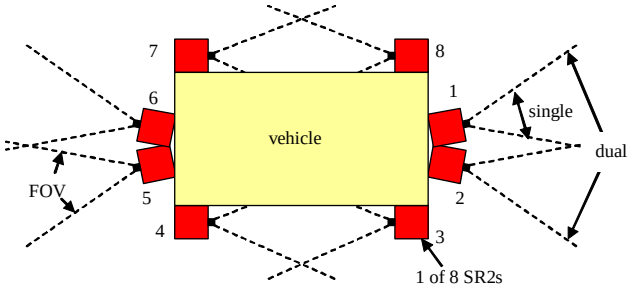

Figure 8 *- Graphic showing one possible configuration of 3D range cameras mounting locations to detect not only in front of the vehicle but, also to the sides.*

Data was collected with two 3D cameras and is shown in Figure 9. Figure 9 (a) shows a photograph of a scene using the same vertical-post test apparatus as shown in Figure 2(a). It was placed at approximately 0.8 m (30 in) above the floor between a table (left) and a desk (right). The 3D camera was at approximately 1 m (39 in) above the floor. The two images were merged in real-time such that the left and right 3D cameras can be viewed as a single image. The processed image was colored slightly different so the operator could distinguish between the two camera responses. Clearly, objects within the scene, including a small crane model on the left can be determined as objects. Ideally, as graphically shown in Figure 8, additional cameras can be joined together to provide an even larger field of view surrounding the vehicle.

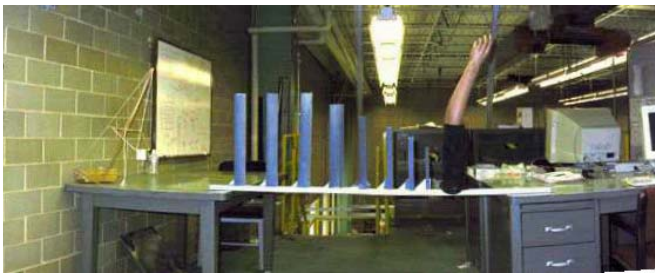

(a)

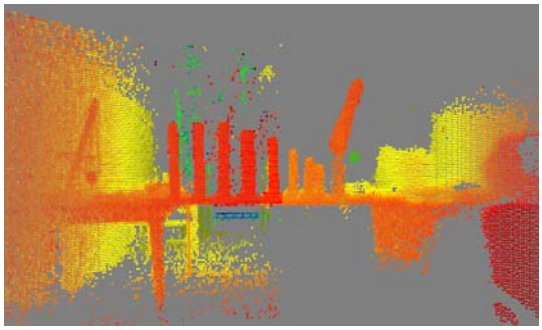

(b)

(c)

Figure 9 *– (a) Photo of a test scene, (b) 3D range camera image from two, merged cameras, and (c) segmented objects. The left and right cameras processed data are shown with different colors to allow the operator to easily understand each camera's data.*

B. Outdoor daylight tests and results

In an effort to move beyond typical indoor AGV applications toward increased robot navigational intelligence, the sensor was taken outdoors. Moving vehicles from indoors to outdoors could open a wide area of applications where safety sensors may become necessary and require alternative sensing capability. For example, AGV applications could include material handling from indoors to outdoors to a staging area or into another building. The shipbuilding industry typically has long, narrow facilities along water, potentially supporting the need for autonomous vehicles carrying a variety of part sizes and shapes and navigating around people, clutter, buildings, and other vehicles. Safety of people and equipment is a large concern and will require sensors capable of sensing through all weather and light conditions to which the vehicle is exposed as well as from indoor lighting or outdoor shade to full sun no matter what time of day the vehicle is functional.

Although the 3D range camera manufacturer has stated that the camera is currently only reliable when used during indoor lighting conditions, the authors felt that a minimal inclusion in this paper is relevant to current AGV applications and provides the reader with a broader scope of future sensor applications. Replacing the LEDs (light emitting diodes) on the camera with laser diodes may improve the bright lighting condition challenges. We took the LED camera outdoors during reduced daylight conditions. The conditions were

cloudy (full overcast) and the robot supporting the sensor was positioned in the shade beneath leaf-covered tree branches. The experiment therefore, began addressing outdoor lighting and object detection issues, such as sensing objects that are potentially recognizable without fully exhausting all outdoor light conditions.

Figure 10 shows a photo of a large tree trunk and branches along with 3D range information from the camera positioned about 2.5 m away. The rear, right branch also shows a clear difference in range data toward 3.5 m where it measures, using a ruler, approximately 1 m behind the front, center branch. Objects behind the tree are approximately a minimum of 14 m away and the ground incrementally approaches in range from 1 m to 2.5 m between the camera and the tree as the range data shows. Notice the similarity of the tree in the photo to the range and segmented data where range information about the tree is accurate to within several centimeters. This accuracy is left somewhat vague as the tree has a very irregular surface and shape. And since the manufacturer states that the camera has range accuracy to within 5 mm, the authors feel that the data is valid.

Similarly, Figure 11 shows a photo of the corner of a building along with the 3D range information, again from about 2.5 m away. In this case however, the sun was shining brighter on the left side while more shaded on the right. Similar to the tree data, the corner range data was accurate to within a few centimeters. Although the sharp corner is indecipherable perhaps due to the angle of reflection being approximately 45°, there is definite range response from the camera showing that a large object is in front of the robot regardless of the bright/shaded light conditions. Some small detail can also be picked out of the building corner range data as the right side brick, from the corner to 43 cm away from the corner, is recessed by 1.5 cm and the recess is visible in the data as a vertical line. However, an algorithm to determine this line from the overall corner data may be difficult to design.

(a)

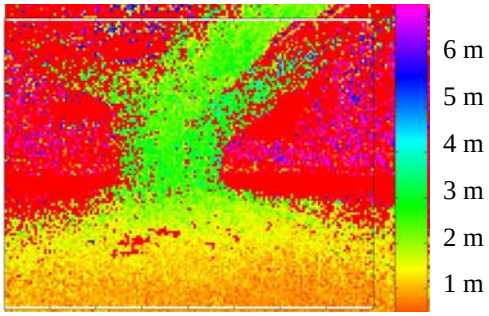

(b)

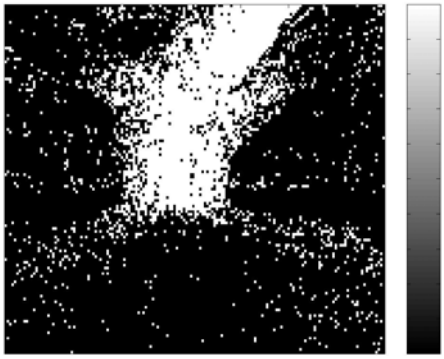

(c)

Figure 10 (a) shows a photo of a tree and (b) shows 3D range information and (c) shows segmented data about the tree with respect to the camera.

V. SUMMARY AND CONCLUSIONS

This paper describes an obstacle detection and segmentation algorithm for Automated Guided Vehicle (AGV) navigation in factory-like environments using a novel 3D range camera. The range camera is highly attractive for obstacle detection in industrial applications as it will be relatively inexpensive and can deliver range and intensity images in real-time. The performance of the 3D range camera was evaluated by comparing it with ground truth provided by a single-line scanning laser rangefinder.

A concept for sensor mounting was also described with corresponding data collected and represented for combining two or more sensors for a larger sensor FOV. Also, a sensor modulation issue was described with a suggested remedy to allow objects beyond the 7.5 m modulation distance to be known or eliminated from the data. We have taken and analyzed some outdoor data and the preliminary results show good promise in using this sensor for outdoor forest environments, in other areas that are shaded, and in night conditions.

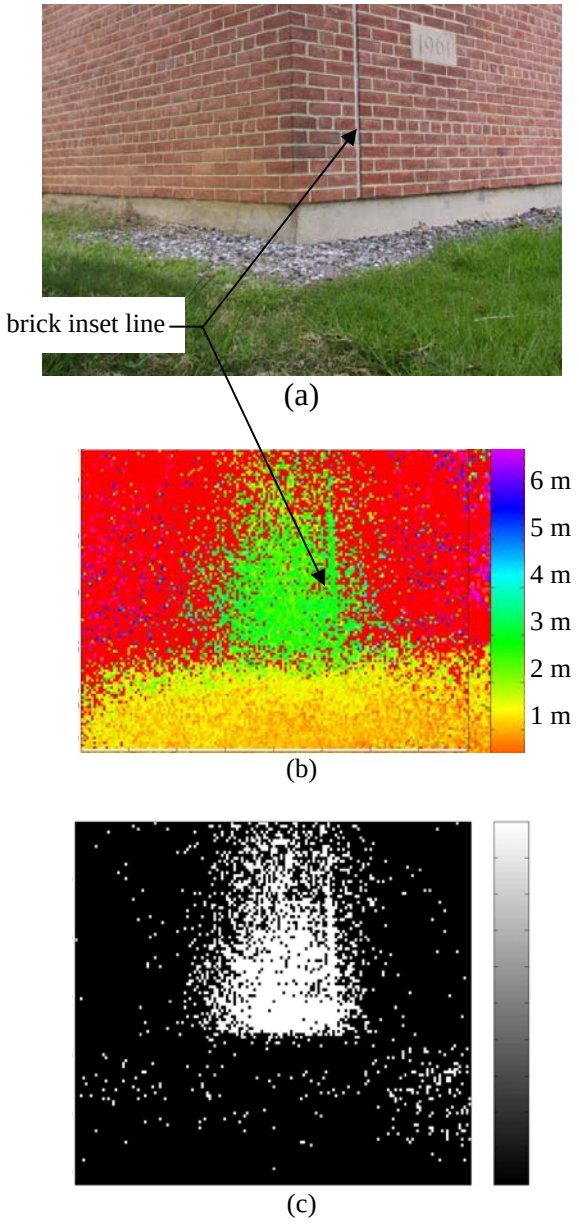

Figure 11 *(a) shows a photo of the corner of a building and (b) shows 3D range information and (c) shows segmented data about the corner with respect to the camera. Note how the corner is not distinctly defined, except for the vertical inset brick line on the right, although clearly a large object (corner) is evident in the data.*

We envisage the extension of the work detailed in this paper toward:

- moving obstacle detection from a moving AGV for indoor applications,
- combining the sensor with a color camera for detecting and tracking obstacles over long distances, and
- outdoor environments.

Some prospective applications include: mapping factory environments ("lights-out") manufacturing inside and outside during night (dark) hours, and even for use in space due to its lightweight and compactness.

VI. ACKNOWLEDGEMENTS

The authors would like to thank Peter Russo, student worker from the University of Maryland, for his contribution of dual, 3D camera sensor processing. Also, the authors thank John Gibbons, Transbotics Corp. for suggesting the study of wrap-around mounted sensors.

VII. REFERENCES

[1] P. Batavia and S. Singh. Obstacle Detection Using Adaptive Color Segmentation and Color Stereo Homography. In Proc. of the IEEE Intl. Conf. on Robotics and Automation, May 2001.

[2] M. Bertozzi, A. Broggi, A. Fascioli, and P. Lombardi. Artificial Vision in Road Vehicles. In Proc. of the 28th IEEE Industrial Electronics Society Annual Conf., 2002.

[3] T. Chang, T-H. Hong, S. Legowik, and M. Abrams. Concealment and Obstacle Detection for Autonomouos Driving. In Proc. of the Intl. Association of Science and Technology for Development - Robotics and Application, 1999.

[4] A. Ewald and V. Willhoeft. Laser Scanners for Obstacle Detection in Automotive Application. In Proc. of the Intell. Vehicles Symp., 2000.

[5] J. Hancock, M. Hebert, and C. Thorpe. Laser Intensity-based Obstacle Detection. In Proc. of the IEEE/RSJ Intl. Conf. on Intelligent Robots and Systems, 1998.

[6] M. Hariti, Y. Ruichek, and A. Koukam. A Voting Stereo Matching Method for Real-Time Obstacle Detection. In Proc. of the IEEE Intl. Conf. on Robotics and Automation, 2003.

[7] Hecht, Eugene, Optics, Schaum's Outline Series, McGraw-Hill ,1975

[8] T-H. Hong, T. Chang, C. Rasmussen, and M. Shneier. Feature Detection and Tracking for Mobile Robots Using a Combination of Ladar and Color Images. In Proc. of the IEEE Intl. Conf. on Robotics and Automation, May 2002.

[9] T. Hong, R. Bostelman, and R. Madhavan, Obstacle Detection using a TOF Range Camera for Indoor AGV Navigation, PerMIS 2004, Gaithersburg, MD, June 2004.

[10] T. Oggier, M. Lehmann, R. Kaufmann, M. Schweizer, M. Richter, P. Metzler, G. Lang, F. Lustenberger, and N. Blanc. An All-solidstate Optical Range Camera for 3D Real-time Imaging with Subcentimeter Depth Resolution. In Proc. of the SPIE Conf. on Optical System Design, September 2003.

[11] C. Olson, L. Matthies, H. Schoppers, and M. Maimone. Robust Stereo Ego-motion for Long Distance Navigation. In Proc. of the IEEE Intl. Conf. on Computer Vision and Pattern Recognition, 2000.

[12] K. Owens and L. Matthies. Passive Night Vision Sensor Comparison for Unmanned Ground Vehicle Stereo Vision Navigation . In Proc. of the IEEE Intl. Conf. on Robotics and Automation.

[13] N. Sgouros, G. Papakonstantinous, and P. Tsanakas. Localized Qualitative Navigation for Indoor Environments. In Proc. of the IEEE Intl. Conf. on Robotics and Automation, 1996.

[14] R. Williamson and C. Thorpe. A Trinocular Stereo System for Highway Obstacle Detection. In Proc. of the IEEE Intl. Conf. on Robotics and Automation, 1999.

[15] American Society of Mechanical Engineers' Safety Standard for Guided Industrial Vehicle and Automated Functions of Manned Industrial Vehicle. Technical Report ASME B56.5, 1993.

[16] British Standard Safety of Industrial Trucks - Driverless Trucks and their Systems. Technical Report BS EN 1525, 1998.